Macro and Micro Rate Zonal Analytical Centrifugation of Polydisperse and Slowly Diffusing Sedimenting Systems in Isovolumetric Density Gradients. Application to Cartilage Proteoglycans†

Francisco J. Müller, Candido F. Pezon, and Julio C. Pita*

Department of Medicine, School of Medicine, University of Miami, Miami, Florida 33101, and Veterans Administration Medical Center, Miami, Florida 33125

Received August 18, 1988; Revised Manuscript Received January 12, 1989

ABSTRACT: A method to study the polydispersity of zonally sedimenting and slowly diffusing macromolecules or particles in isokinetic or isovolumetric density gradients is presented. First, a brief theory is given for predicting the zonal profile after a "triangular" (or "inverse") zone is centrifuged. This type of zone is essential to preserve hydrodynamic stability of the very slowly diffusing polydisperse solutes. It is proven, both by semitheoretical considerations and by computer calculations, that the resulting concentration profile of macrosolute is almost identical with that obtainable with a rectangular zone coextensive with the triangular one and carrying the same total mass. Next, practical procedures are described for the convectionless layering of very small triangular zones (50 μL or less). The linearity and stability of the zones are experimentally tested and verified. Finally, the method is applied to cartilage proteoglycan preparations that included either the monomeric molecules only or both the monomeric and the aggregated ones. The zonal results are compared with those obtained by using conventional boundary sedimentation. The two sets of results are seen to coincide fairly well, thus proving that the present technique can add to preparative zonal centrifugation the analytical precision of boundary sedimentation. A multimodal polydisperse system is suggested to describe the aggregated proteoglycan macromolecules.

Centrifugal analysis of macromolecules is usually done by performing classical boundary sedimentation either in the analytical (optical) ultracentrifuge (Schachman, 1959) or in the preparative centrifuge by means of the transport method (Pita et al., 1978). For preparative purposes, on the other hand, a most commonly used method is rate zonal centrifugation, again either in the zonal centrifuge originally introduced by Anderson (1955) or in regular swinging bucket cells provided with means for extracting the contents at the end of centrifugation (Anderson, 1962; Griffith, 1976; Ridge, 1978). Although zonal centrifugation has received great theoretical attention and quantitative improvements in recent years (Price, 1974; Hsu, 1976; Steensgard et al., 1978), its reliability and precision to combine in a single experiment both the preparative and analytical applications still has not been completely achieved. This is especially true for those particular cases in which the macromolecules are heavy (MW > 10^6) and polydisperse (for example, DNA, viruses, and proteoglycans). This type of molecule is usually hardly or very slowly diffusing (typically $D = 10^{-7}$–10^{-8} Ficks). As a result, the well-known phenomenon of "droplet sedimentation" (Schumaker, 1967; Sartory, 1969; Halsall, 1971; Halsall & Sartory, 1976) might take place, thus endangering the hydrodynamic stability of the molecules and, therefore, defeating the analytical precision of the method. Hence, either the zone capacity would have to be considerably reduced (thus in turn impairing the preparative purposes, especially when only microvolumes of the sample are available) or a more stable initial zonal profile would have to be used. The latter alternative could consist, for example, in using the so-called "inverted" or "triangular" zone first introduced by Britten and Roberts years ago (1960). A difficulty with this type of zone, however, is the lack of theory for correlating the zonal shape and its progressive spreading during centrifugation with the sedimentation coefficient distribution function, $g(S)$, which in our case (negligible diffusion) practically governs in its entirety such spreading during centrifugation.

In this paper we will outline a theoretical development for the determination of the $g(S)$ function both in the triangular zone and in the more commonly used rectangular ones. A rigorous theory for the triangular case, however, would be practically impossible if, as usually happens in zonal centrifugation, the S values are a nonlinear function of the changing density and viscosity values of the required supporting medium underlying the zone. Previous attempts to obtain $g(S)$ distributions in this way by zonal centrifugation have only been approximate (Halsall & Schumaker, 1969), with the need of ultimately resorting to the analytical centrifuge for $g(S)$ estimation and to empirical plots of S values versus density and viscosity along the cell.

In this paper we will resort, rather, to the elegant isokinetic and isovolumetric density gradients introduced in a previous work (Pita and Müller, 1985), which yield the S values as linear functions of the radial positions (or volume fractions) along the cell. These gradients are as easy to prepare as the linear ones and will greatly simplify the theory of the triangular zonal shape as a function of any arbitrary $g(S)$ distribution. Reciprocally, the theory will allow determination of the $g(S)$ function from an experimentally determined final concentration profile of an initially triangular zone. In the experimental part of this paper the theory will be tested by applying it to polydisperse proteoglycan Al and AlDl preparations from articular cartilage. Special consideration will be given to the handling of microvolumes and the production of triangular zones of 50 μL or less. The theory, however, can be applied

† This work was supported by the Veterans Administration Funds and by the National Institutes of Health, Grants AR 38733 and AM 33854.

0006-2960/89/0428-5276$01.50/0

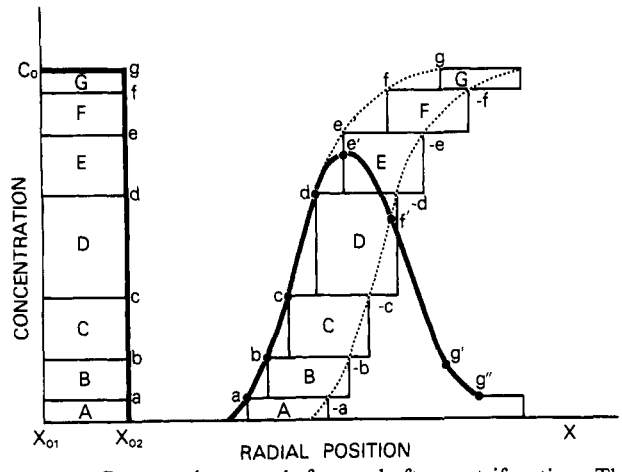

FIGURE 1: Rectangular zone, before and after centrifugation. The resulting bell-shaped curve (solid line) is the difference of the dotted lines representing two fictitious boundary centrifugations starting at X_{01} and X_{02}, respectively. C_0 is the initial concentration. The rectangles represent the masses (areas) of single components A, B, C, ... within the distribution of S values.

generally to any zonal volume range.

Theory

If an infinitely thin lamella of a nondiffusible polydisperse system of macromolecules or particles is zonally centrifuged, it seems intuitively evident that the resulting macromolecular concentration profile should be linearly proportional to the S value distribution function, $g(S)$, characterizing the system in the zone. Hence, a bell-shaped or Gaussian-like curve should result. Such "thin band" approximation commonly employed in the theory of zonal centrifugation, however, would preclude the detailed comparison of rectangular and triangular zones which, of necessity, ought to be considered as finite and as having a certain width, ΔL, extending from the air–liquid meniscus at X_{01} to the point of contact with the supporting gradient, X_{02}. In the following treatment real-sized (finite) zones will be considered. First, the rectangular zone will be analyzed as a whole, and then treatment will be extended to the triangular zone by simply considering subzones of linearly decreasing concentrations.

Theory for the (Polydisperse) Centrifugal Spreading of a Rectangular Zone and g(S) Determination Thereof. Figure 1 represents a graphical method for predicting the concentration profile for a rectangular zone initially layered at the left between the said radial positions X_{01} and X_{02}. The sedimenting components are depicted as rectangles of mass (areas) A, B, C, ..., respectively. The lower rectangles are arbitrarily made to correspond to the slow species and the upper ones to the faster species. In reality, of course, all rectangles are "mixed" within the same zone volume. The small letters represent the cumulative masses (or concentrations). So, $a = A$, but $b = A + B$, $c = A + B + C$, and so on. At the right the rectangles are shown displaced relative to each other after centrifugation has occurred, each one having advanced a distance proportional to its constituent S value. The rectangles' sizes are shown to remain constant, since no radial dilution occurs in isovolumetric gradients. By simple inspection of Figure 1, it can be seen that the first points, a–d, of the resulting curve (solid line) are identical with those of a regular sedimentation boundary; i.e., they are the progressive summations of components A, B, C, etc. At point e, however, the slowest component, A, has already vanished. Hence, an amount a must be subtracted from point e to get the observed point e'. In the same fashion, from the cumulative point f an amount c must be subtracted to obtain the observed point f'. This subtraction is repeated every time a component vanishes until g'' is reached, where only component G (the fastest one), remains. This process is equivalent to subtracting from each point a–g along the upper boundary (dotted line) the values $a, b, \ldots f$, lying along the dotted boundary underneath. Both boundaries can be conceived as fictitious centrifugal profiles resulting from flat boundaries that started sedimenting at X_{01} and X_{02}, respectively. The actually observed curve will be, therefore, the numerical difference between these two fictitious boundaries.

When the previous intuitive result is translated into analytic terms, the concentration C_X for any point X under the final zonal profile can be expressed as the difference between the two integral functions $G(S_{01})$ and $G(S_{02})$ that can be derived from the (classical) sedimenting boundaries that started at X_{01} and X_{02}, respectively. Hence

$$C_X/C_0 = G(S_{01}) - G(S_{02}) \tag{1}$$

In eq 1 division by the initial concentration C_0 in the rectangular zone implies that the $G(S)$ functions have been normalized to unity. The simplicity of this equation is possible precisely because in isovolumetric gradients in sectorial cells (or isokinetic gradients in cylinders) no dilution of the plateau occurs and, hence, the boundary is represented faithfully by the integral $G(S)$ function defined, as usual, by

$$G(S) = \int g(S)\, dS \tag{2}$$

where, in turn, $g(S)$ is defined as

$$g(S) = dC/dS \tag{3}$$

In experimental centrifugal determinations where the C_X/C_0 profiles are analyzed at discrete X points separated by intervals ΔX, each of volume ΔV, the integral eq 2 can be replaced by the finite difference equation

$$\Delta G(S) = g(S)\Delta S \tag{4}$$

where $g(S)$ is the average differential distribution function at some middle point between X and $X + \Delta X$. We notice, then, that the difference $G(S_{01}) - G(S_{02})$ of eq 1 can yield the $g(S)$ function if divided simply by ΔS as implied by eq 4. The coefficients S_{01} and S_{02} and the range ΔS can be related by the linear formula for S values in isokinetic gradients in cylinders [eq IVA of Pita et al. (1985)]. By use of this formula for contiguous aliquots N and $N - 1$

$$S_N = N\Delta X/X_{01}\omega^2 t \tag{5A}$$

and

$$S_{N-1} = (N - 1)\Delta X/X_{01}\omega^2 t \tag{5B}$$

subtracting

$$\Delta S = S_N - S_{N-1} = \Delta X/X_{01}\omega^2 t \tag{6}$$

Likewise, the different arguments S_{01} and S_{02} in eq 1 correspond to the coefficients

$$S_{01} = (X_N - X_{01})/X_{01}\omega^2 t \tag{7A}$$

and

$$S_{02} = (X_N - X_{02})/X_{01}\omega^2 t \tag{7B}$$

again subtracting

$$S_{01} - S_{02} = (X_{02} - X_{01})\omega^2 t = \Delta L/X_{01}\omega^2 t \tag{8}$$

indicating that S_{01} is bigger than S_{02} precisely because the S_{01} molecules have traveled, to reach the same point X_N, a distance bigger than the one traveled by S_{02} molecules, the excess being

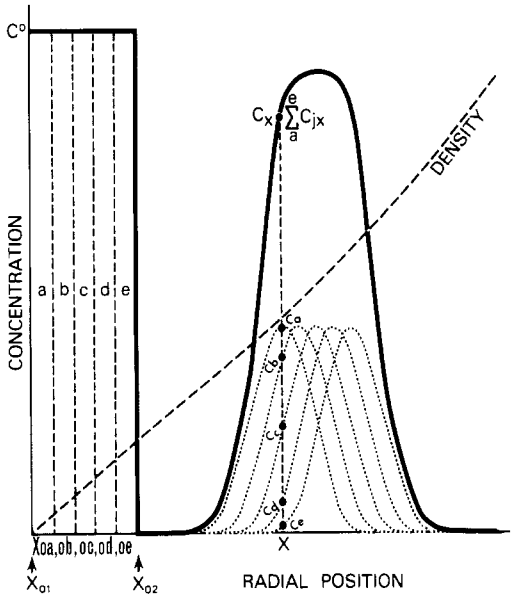

FIGURE 2: Rectangular zone subdivided into infinitesimal plane elements. The resulting bell-shaped curve (solid line) is the addition (not shown to scale) of all the dotted-line curves. The latter represent the individual profiles generated by each element after certain time of centrifugation. Each plane element contains a complete distribution of S values, $g(S)$. The supporting density gradient (– – –) is shown to be continuous across the zone interface, X_{02}.

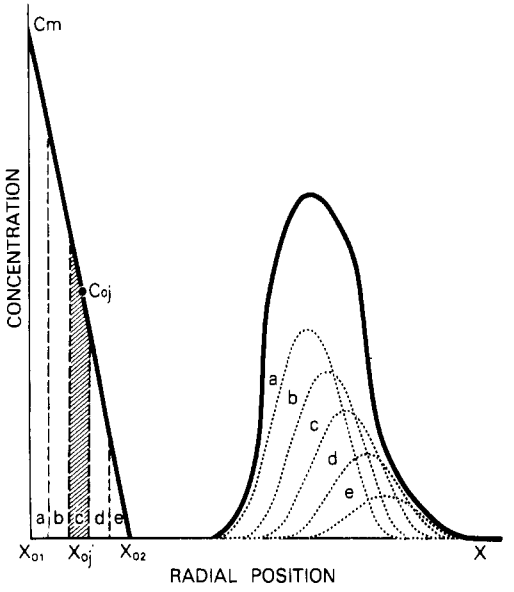

FIGURE 3: Triangular zone before centrifugation (left) and after centrifugation (right). The latter is the summation (not drawn to scale) of the bell-shaped (dotted line) curves having decreasing peaks. Subband c, initially located at the midpoint, X_{0j}, has been marked out, just to illustrate its initial concentration, C_{0j}, as being equal to $C_m/2$.

equal to the bandwidth $X_{02} - X_{01} = \Delta L$.

Now, if the intervals for analysis, ΔX, are made equal, by stipulation, to the bandwidth ΔL, then the difference in eq 1 due to the displacement between the two meniscuses can be translated as a difference for a single meniscus but different aliquots, N and $N - 1$, eq 6. In other words

$$G(S_{01}) - G(S_{02}) = G(S_{01})_N - G(S_{01})_{N-1} \quad (9)$$

Dropping the subscript 01 in the right-hand side of eq 9 and substituting it into eq 1, we get

$$C_{\tilde{N}}/C_0 = G(S)_N - G(S)_{N-1} \quad (10)$$

where the subscript $\tilde{N}$ represents some middle point between N and $N - 1$. Then the approximation of eq 4 can be combined with eq 10 to yield

$$g(S)_{\tilde{N}} = C_{\tilde{N}}/C_0\Delta S \quad (11)$$

or, if the ΔS of eq 6 is used

$$g(S)_{\tilde{N}} = (C_{\tilde{N}}/C_0)(X_{01}\omega^2 t/\Delta X) \quad (12)$$

The remarkable simplicity of the previous equation confirms our initial intuition that the concentration profile, $C_{\tilde{N}}/C_0$, is linearly related to the $g(S)$ distribution function of S values. Now it remains to see the effect of using a triangular instead of an initially rectangular zone.

Extension of the Previous Theory to the Initially Triangular Zone. A possible way to compare the centrifugal behavior of the triangular and rectangular zones would be to subdivide each type of zone not into S-value groups as in Figure 1 but into very thin (rectangular) subzones as shown in Figures 2 and 3. In this case each subzone will contain the whole $g(S)$ distribution of S values. Then the individual profiles due to each subzone would follow the bell-shaped (dotted) curves also shown in the figures after some centrifugation time has passed. Obviously these curves are displaced according to their initial positions, X_{0a}, X_{0b}, ... X_{0e}, but each one follows the same pattern, as demanded by eq 12. Then the resulting concentration at a given point X would be the addition of each individual concentration C_a, C_b, ... C_e due to each component profile wherever these profiles happen to be located. The solid curve represents the resultant of all the additions for all points X (not drawn to scale).

An identical reasoning can be applied to the triangular zone (Figure 3) except that now the "strength" or initial concentration of each subzone will decrease linearly as we move from X_{01} to X_{02}. Likewise, the component (dotted line) curves a, b, ... e, after centrifugation, are shown as progressively diminishing toward the right. The question is, then, how do the resulting total profiles (solid lines in Figures 2 and 3) compare with each other?

An analytical theory for this problem using integration of all the contributing bell-shaped curves in both types of zones requires the representation of those curves by some kind of integrable analytic function. Unfortunately, the most obvious choice, the Gaussian error function, Ne^{-u^2}, cannot be so integrated. We have used Gaussian-like functions such as $(\sin u^2)/u^2$ and have obtained complicated integrated equations for the triangular case. These equations are difficult to compare with the rather simpler equations obtainable for the rectangular case. A numerical approach, however, is most instructive and can be easily developed by computerized serial additions of the various subzonal profiles. Using the Gaussian error function as generating the fundamental $g(S)$ distribution profile, we adapted the u^2 variable as

$$g(S) = g_{max}e^{-u^2} \quad (13A)$$

with

$$u = (S - S_p)/S_{min} \quad (13B)$$

where S_p is the "peak" or average S value in a symmetric (Gaussian) distribution in which the extremes are S_{min} and S_{max} (i.e., $S_p = (S_{min} + S_{max})/2$). The actual S_{min} and S_{max} values used were 10 and 50 S, respectively, which simulated, more or less, the range for a large proteoglycan monomer distribution. With $S_p = 30$, the extreme u values were −2 and 2, thus "cutting" the error function at 1.8% of its maximum ordinate, g_{max}.

The zones were divided into four subzones, 1 mm each, extending from $X_{01} = 60$ to $X_{02} = 64$. The total X range was

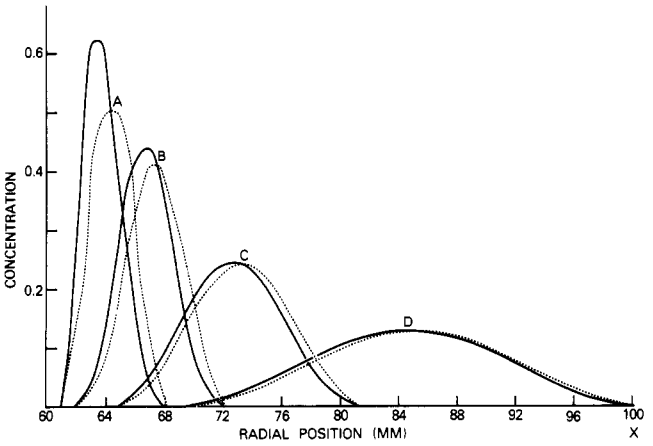

FIGURE 4: Computer-calculated zonal profiles. Triangular (—) and rectangular (···) zonal profiles are shown for four progressive $\omega^2 t$'s: (A) 1.65×10^{10}; (B) 3.3×10^{10}; (C) 6.6×10^{10}; (D) 13.3×10^{10}. The initial zones, extending from $X = 60$ mm to $X = 64$ mm are not shown.

60–104 mm. Then four different $\omega^2 t$ parameters were used in eq 5A, namely, 1.65, 3.3, 6.6, and 13.2 (by 10^{10} in all cases). The resulting four sets of S_{01} values were plugged into the S variable eq 13B, the corresponding $g(S)$ values calculated, by eq 13A, and finally the C_N/C_0's were obtained via eq 12. For the rectangular zone all subzones had equal "strengths" or initial concentrations of $C_0 = 1$. For the triangular zone the maximum concentration was $C_m = 2$ at X_{01} and the minimum, 0, at X_{02}. Hence, the four triangular subzones were assigned concentrations of 1.75, 1.25, 0.75, and 0.25 at their midpoints. The reason for this choice was to have equal total masses (areas) under both the triangular and rectangular zones.

The numerical results are plotted in Figure 4 for the four $\omega^2 t$'s chosen, A, B, C, and D. It is immediately seen that the two types of zones, which initially are very dissimilar (stage A), converge to the same type of profile for stages C and D. The maximum ordinates, for example, differed by 3% in stage C and only by 0.5% in stage D. It can be safely concluded that for a sufficiently large $\omega^2 t$ both types of zones yield undistinguishable concentration profiles. How much is "sufficiently large" depends upon the zone spreading relative to the initial zone width. If the results of Figure 4 can be generalized, it might be said that after a polydispersity spreading equivalent to four zone widths (case C) or more (case D), the agreement between both types of zones is practically acceptable within a 3% or even smaller error.

Furthermore, when the average horizontal displacement or X differences between equal ordinates of the two curves for each run was computed, it was consistently found to be equivalent to one-sixth of the initial zone width (0.66 mm in our case). This happens because the baricenter of the triangular zone at the origin is shifted centripetally with respect to the rectangular baricenter precisely by one-sixth of the zone width. Hence, a practical advantage can be taken of this fact when the $g(S)$ values are determined via the C_N/C_0 points of a triangular profile: the observed C_N points are shifted centripetally (down the cell) by one-sixth of the initial bandwith. Then they can be used in connection with eq 12 as if they had originated from a rectangular zone carrying the same mass instead of a triangular one. (See Results for illustration of details.)

Experimental Procedures

All the reagents used for the concentration determination of proteoglycans by the modified carbazole method of Bitter and Muir (1962) were of analytical grade and were supplied by Mallinckrodt Inc. (Paris, KY). The cesium sulfate for the gradients came from Gallard-Schlesinger Chemical Corp. (Carle Place, NY). The proteoglycan AlDl preparation (monomers) and Al (monomers plus aggregates) were obtained from dog articular cartilage and from rat chondrosarcoma, respectively, by the extraction and purification methods of Sajdera and Hascall (1969). The AlDl preparation was further purified by standard zonal centrifugation. Coefficients bigger than 30 S were discarded since these higher species consist mainly of self-associated monomers that tend to sediment anomalously faster with increasing rotor speeds in isovolumetric gradients (Pita and Müller, unpublished observations).

The polycarbonate sectorial cells, of 1.5-mL capacity, have been described by Pita et al. (1983). For bigger volumes (12 mL), ordinary cellulose cylindrical tubes were used. The ultracentrifuge used was an OTD-2 Sorvall with acceleration rate control, electronic $\omega^2 t$ integrator, and titanium swinging bucket rotors, always operated at 20 °C. A peristaltic Sigmamotor pump (Middleport, NY), Hamilton syringes, aluminum cams (described below), miniature T-connections from Durrum (Palo Alto, CA) holding only 3 μL on each arm, very thin polyethylene tubing from Clay Adams (Parsippany, NJ), and manipulators were employed for gradient preparation.

Boundary Centrifugation. For comparative purposes the same PG preparation to be studied by the new zonal methodology was also analyzed by classical boundary sedimentation in a small linear stabilizing gradient as described by Pita et al. (1978). To minimize the different ways in which concentration dependence effects might alter the boundary profile when compared with the zonal one, the boundary initial concentration was chosen at an intermediate value between the zonal initial and final peak concentrations.

Preparation and Layering of Triangular Zones of Very Small Volume. In principle, a triangular zone can be easily prepared by using any commercially available linear gradient mixer. The solute and supporting medium of density ρ_{01} are separately placed in the two compartments of the mixer. In this way two mutually opposed linear gradients are generated. By minimizing the amount of solution in each compartment (say, 0.25 mL) small zones can be produced. Further reduction, however, becomes impossible for the proper stirring and draining of the mixer. For much smaller zones (say, 50 μL or less), a special but inexpensive gradient mixer was made with two 50-μL Hamilton syringes, each one loaded with a volume of 25 μL. The complete setup is shown in Figure 5. The syringes are mounted in a lucite block (LB), and their plungers are moved with two cams (CA and CB), which in turn were affixed to the axis PP′ of a peristaltic pump capable of very slow rotation. Insert C is a top view of the two superimposed cams, and their precise shapes are described by the equations given in the figure's legend. The two solutions become mixed at the central point of a miniature T-connection (M), and the zone is layered through tip N onto the supporting medium W inside a polycarbonate sectorial cell (or in a regular cylindrical cell).

Between N and W a small piece of wettable paper (for example, dialyzing paper) is glued as illustrated in insert B of Figure 5. This wetted paper acts as a carrier of the solution to be layered. As a result, the zone is seen to flow onto the gradient without any perceptible convection. The cell is held with a manipulator clamp MC to be very slowly lowered while the zone is layered so that the tip N never dips into the zone more than 0.5 mm. Air bubbles, of course, are to be avoided, and to this purpose the discharge polyethylene tubing should be filled with gradient solution prior to layering. Ideally this

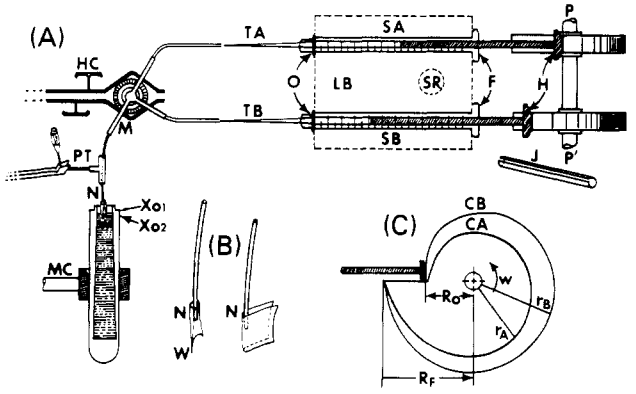

FIGURE 5: Experimental setup for producing and layering very small triangular zones. (A) LB, lucite block; SA, SB, Hamilton syringes with flanges, F, rounded plunger heads, H, tips, TA and TB, held in position with O-rings, O; PP′, peristaltic pump axis; J, cylindrical jacket with longitudinal slot to secure plungers in fixed position when desired; M, miniature T-connection (3 μL in each arm), encroached in a plastic tube held with clamp HC; PT, positioning T attached to a twisted syringe needle held with small prongs to guide polyethylene discharge tubing MN. Manipulator clamp, MC, holds the centrifugation cell and lowers it during layering. NW is a small piece of dialyzing paper glued to tip N as shown in insert B. (B) Rectangular piece of dialyzing paper folded and fixed to tip N with traces of instant glue, trimmed with baby scissors into an open conical shape as shown. (C) Cams, CA and CB, affixed to axis PP′ of driving motor. The smallest, R_0, and largest radii, R_F, are equal for both cams. The intermediate radii, r_A and r_B, however, increase with rotational angle w and time t according to the following equations: $r_A = R_0 + (\Delta R/T^2)t^2$ and $r_B = R_0 + 2(\Delta R/T^2)t^2 - (\Delta R/T^2)t^2$, where T is the rotation period and $\Delta R = R_F - R_0$. In this paper, $R_0 = 3$ cm and $R_F = 6$ cm, and T usually was about 45 s.

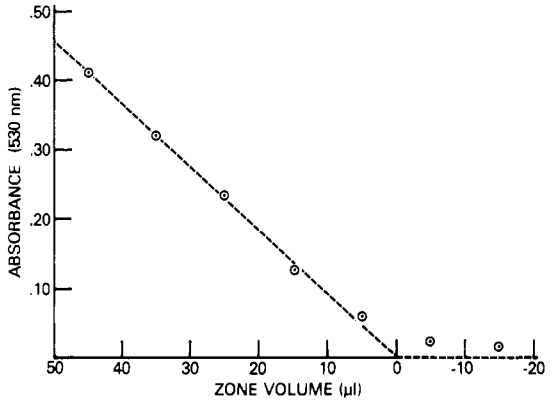

FIGURE 6: Triangular zonal profile analyzed before centrifugation.

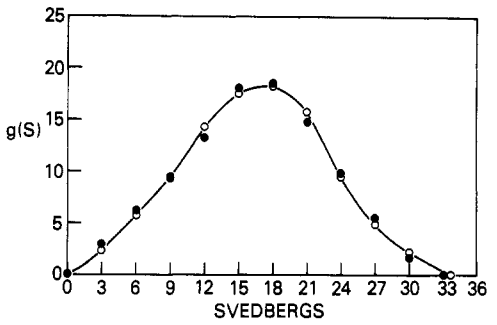

FIGURE 7: Comparison of zonal and boundary centrifugation of a proteoglycan monomeric preparation. The vertical axis in arbitrary units is proportional to both concentration and $g(S)$ function. The S value axis (in Svedberg units) is obtained from the aliquot number N and eq 7A. The solid line is a computer-drawn curve through the open circle points corresponding to the triangular zonal centrifugation. The solid circles are the superimposed discrete values corresponding to the boundary sedimentation of the same proteoglycan monomeric preparation.

solution should have the topmost density of the underlying column, say ρ_{02} (corresponding to position X_{02}), or perhaps even a slightly smaller value, ρ_{02}', so that the small discontinuity, $\rho_{02}-\rho_{02}'$, acts in favor of stabilizing the zone. A practical way to assure these conditions is to fill the cell up to position X_{01} when the supporting gradient is first delivered into it and then withdrawing from this gradient a volume V equivalent to that of the zone, thus emptying the length $X_{02} - X_{01}$ out of the cell. This volume is homogenized and is used to fill syringe SB, the lower one, for the preparation of the triangular zone. In this way an average density $(^1/_2)(\rho_{01} + \rho_{02})$, smaller than ρ_{02}, will be guaranteed for the zone formation.

A last practical detail must not be overlooked when such small volumes are used. Sections MTA and MTB offer no problem provided they are completely filled with the solution of their respective syringes. But section MN will retain, at the end of the mixing process, part of the zone that has to be layered. This residual volume can be discharged by pushing carefully by hand an equivalent volume RV out of the sedimenting particle solution in SA at the end of the layering process.

Results

Verification of Zone Shape and Stability before Centrifugation. A triangular zone consisting of 50 μL of the preselected proteoglycan monomer (AlDl) preparation at a concentration $C_m = 2$ mg/mL was layered and recovered after 10 min without centrifugation. Five 10-μL aliquots were withdrawn plus two 10-μL layers from the underlying gradient. The aliquots were analyzed for hexuronate concentration, and the results are plotted in Figure 6. The linearity was excellent as judged by the correlation coefficient of 0.998 obtained when the points were fitted to a straight line. The values at −5 and −15 corresponding to the underlay had only trace amounts of proteoglycan, indicating that droplet sedimentation was virtually absent. Longer waiting times did not change appreciably the results. Initial C_m concentrations of 3 mg/mL were also possible for proteoglycans. For rectangular zones, however, even a concentration of 1 mg/mL was unstable, at least for the medium densities used at X_{01} and X_{02} in our experiments (1.013 and 1.026 g/cm^3), respectively.

Comparative Zonal and Boundary Sedimentations of AlDl Proteoglycans. The same proteoglycan monomer preparation of the previous test was zonally centrifuged in the sectorial cell of 1.5-mL capacity but at a smaller concentration (0.7 mg/mL). The supporting gradient was prepared by mixing a 29.3% solution of Cs_2SO_4 with 0.69 mL of buffer (ρ = 1.013 g/cm^3) in Noll's chamber (Pita et al., 1985). The triangular 50-μL zone was prepared as outlined above by using two 50-μL Hamilton syringes. The tubing MN (Figure 5) had 0.011-in. i.d. and contained 8 μL, so syringe SA was loaded with 50/2 + 8 = 33 μL of proteoglycan solution. The zone was delivered in 45 s. Centrifugation was conducted at 41 156 rpm for 90 min ($\omega^2 t = 10^{11}$), starting at X_{01} = 58.3 mm from rotor center. At the end of centrifugation 25 aliquots (50 μL each) were extracted and analyzed for hexuronate concentration. All concentrations were divided by half the peak concentration (i.e., by $C_m/2$). The ratios were plotted versus aliquot number N, and by use of eq 12 a curve of the $g(S)$ function versus S (eq 7A) was obtained as shown in Figure 7 (open circles).

Comparison with boundary sedimentation was done by running the same sample as described under Experimental Procedures at 40 617 rpm for 60 min ($\omega^2 t = 6.52 \times 10^{10}$ at a concentration of 0.32 mg/mL). (This value fell in between the zonal's initial and final peak concentrations, which were

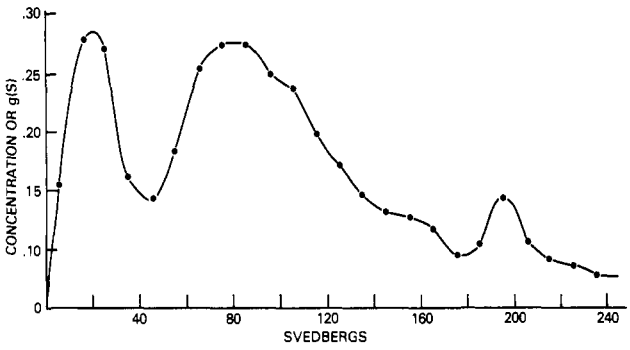

FIGURE 8: Zonal profile of a proteoglycan Al preparation from rat chondrosarcoma. Each aliquot interval corresponded to 10 S. Aggregates correspond to S values greater than 40 S.

0.7 and 0.07 mg/mL, respectively.) The calculated $g(S)$ distribution values are shown also in Figure 7 as solid circles. Agreement with the zonal $g(S)$ curve (open circles) was very good.

Proteoglycan Al Preparation from Rat Chondrosarcoma. This preparation contains, in addition to the proteoglycan monomers, a large amount of proteoglycan aggregates. For adequate resolution of all the aggregated components, the longest centrifugation path available was used. This was the 12-mL cellulose tube mentioned under Experimental Procedures. The triangular zone consisted of 500 μL of the proteoglycan solution at 1.8 mg/mL concentration. Correspondingly, the 24 aliquots extracted after centrifugation were 500 μL each, covering a length of 64.8 mm (2.7 mm per aliquot). The resulting profile (in terms of hexuronate absorbance) is given in Figure 8, and it shows a considerable amount of detail that has never been observed with shorter conventional centrifugation cells. In particular, two populations of aggregated molecules were observed instead of the single aggregated mode reported by researchers that used conventional centrifugal methods or column chromatography.

Discussion

Under Theory of this paper it was presumed that the profile of a thin zone should be proportional to the distribution function $g(S)$ of S values within the zone if only this polydisperse distribution affects the zone's shape (i.e., if diffusion can be neglected). After a brief theoretical elaboration for finite rectangular and triangular zones, the final expression arrived at, eq 12, confirmed our initial presumption. This result is by no means trivial, and it cannot be rigorously demonstrated unless isovolumetric or isokinetic conditions prevail in the sedimenting system. These conditions eliminate plateau dilution and, hence, the fictitious sedimenting boundaries of Figure 1 could be represented by $G(S_{01})$ and $G(S_{02})$ and could be subtracted as done in eq 1 above to obtain the C_X profile for the sedimenting (and spreading) zone. The absence of exponential (plateau dilution) corrections in eq 1 leads to the remarkable simplicity of eq 12.

It is interesting to note that the latter equation can also be generalized to any type of zone coextensive with the rectangular zone and having equal total mass. If two initial profiles so different as a triangle and a rectangle lead to almost identical shapes afer a spreading of four bandwidths has occurred, as demonstrated in this paper, then any intermediate type of sigmoidal curve should also converge to a similar centrifugal profile, provided the total mass is the same. Risk of droplet instability, however, would still depend on how the generalized sigmoidal profile "meets" the supporting gradient at X_{02}. A negative slope, even smaller than in the triangular case, would be ideal. For these reasons, it might not be too important that the layered zone follow a straight line as rigorously as in the example shown in Figure 6. Small imperfections in the cams for preparing the zone, for example, might produce systematic sigmoidal deviations which, for the said reasons, might be within practical tolerance. In this context even approximate triangular formation procedures as crude as that of Williamson (1971) might be justifiable. Here an inclined pipet is first loaded with 0.1 mL of the sedimenting particle solution and then with another 0.1 mL of the supporting medium. Delivery of the contents while the pipet remains inclined will grossly mix the two solutions in a sort of wedge-shaped gradient. Before delivery is done, however, the danger of droplet sedimentation exists inside the pipet, just as in a rectangular zone. In addition, the inclined pipet cannot produce the layering in a way as smooth as the one described in this paper.

It is expected that the smoothness in layering and virtual absence of static and dynamic instabilities in this method lead to $g(S)$ curves comparable or even better than those obtainable by boundary sedimentation. Especially for the faster sedimenting modes the present method offers unique resolution advantages. In boundary sedimentation the faster species, of necessity, lie in the more concentrated regions of the boundary. Hence, these faster modes tend to be masked by the Johnston–Ogston effect. In zonal centrifugation, however, the opposite is true. Here the fastest species find themselves at the leading side of the zone where only supporting medium exists. They are, thus, freer to move, and it is not surprising, therefore, to find such an extended bimodal aggregate distribution as the one observed in Figure 8.

Yet, aggregated macromolecules tend to behave differently from the monomeric ones, in respect to S-value concentration effects and, hence, the coincidence found in Figure 7 with the selected monomers for both types of techniques might not be possible for the bigger aggregated proteoglycans. If this different behavior is due to some intrinsic hydrodynamic property of the aggregates or if it is due to a lack of precise theory for adequately correcting the Johnston–Ogston effect in polydisperse systems (especially when multiple K values are operative) remains yet to be investigated. Efforts in this direction are currently being undertaken in our laboratory.

Qualitatively, however, there is no question that both methods will yield, even for aggregates, the same basic information, for example, in regard to the number of polydisperse families present. In fact, the existence of the bimodal aggregate distribution shown in Figure 8 was first reported by us many years ago (Pita et al., 1979, 1985; Manicourt et al., 1986) while we were still using boundary transport sedimentation. Other researchers, using sophisticated techniques, such as sedimentation fluid flow fractionation (Arner, 1987), have recently confirmed this bimodal aggregate distribution first reported by us and now confirmed with the present zonal technique. The reliability of the present method, therefore, gives credibility to all the details of Figure 8. For example, the shoulders around 110 and 160 S might be true indications of the existence of even more than two modes of proteoglycan aggregation. In fact, some preliminary statistical studies of the aggregation phenomenon seem to indicate that a "multimodal" regime of aggregates is, finally, the true picture of these important cartilage macromolecules in vivo. Efforts to substantiate this hypothesis by means of a computerized aggregating model are now being conducted in our laboratory.

Acknowledgments

We appreciate the chondrosarcoma proteoglycan preparation, a generous gift of Dr. James Kimura, St. Luke Pres-

byterian Hospital, and also the secretarial assistance of Geneva Jackson.

References

Anderson, N. G. (1955) *Science 121*, 775.
Anderson, N. G. (1962) *J. Phys. Chem. 66*, 1984.
Arner, E. C., & Kirkland, J. J. (1987) presented at the annual meeting of the American Rheumatism Association, Washington, DC.
Baldwin, R. L. (1954) *J. Am. Chem. Soc. 76*, 402.
Bitter, T., & Muir, H. M. (1962) *Anal. Biochem. 4*, 330.
Britten, R. J., & Roberts, R. B. (1960) *Science 131*, 32.
Griffith, O. M. (1976) in *Techniques of Preparative, Zonal and Continuous Flow Ultracentrifugation*, Spinco Division, Beckman, Palo Alto, CA.
Halsall, H. B. (1971) *Biochem. Biophys. Res. Commun. 43*, 601.
Halsall, H. B., & Schumaker, V. N. (1969) *Anal. Biochem. 30*, 368.
Halsall, H. B., & Sartory, W. K. (1976) *Anal. Biochem. 73*, 100.
Hsu, H. W. (1976) *Sep. Purif. Methods 5*, 51.
Janado, M., Nichol, L. W., & Dunstone, J. R. (1972) *J. Biochem. 71*, 257-263.
Manicourt, D. H., Pita, J. C., Pezon, C. F., & Howell, D. S. (1986) *J. Biol. Chem. 261*, 5426.
Pita, J. C., & Müller, F. J. (1973) *Biochemistry 12*, 2656.
Pita, J. C., & Müller, F. J. (1985) *Biochemistry 24*, 4250.
Pita, J. C., Müller, F. J., & Howell, D. S. (1975) in *Dynamics of Connective Tissue Macromolecules* (Burleigh, P. M. C., & Poole, A. R., Eds.) Chapter 12, North-Holland, Amsterdam.
Pita, J. C., Müller, F. J., Oegema, T., & Hascall, V. C. (1978) *Arch. Biochem. Biophys. 186*, 66.
Pita, J. C., Müller, F. J., Morales, S. M., & Alarcon, E. J. (1979) *J. Biol. Chem. 254*, 10313.
Price, C. A. (1974) in *Subcellular Particles, Structures, and Organelles* (Laskin, A. I., & Last, J. A., Eds.) Chapter 6, Marcel Dekker, New York.
Ridge, D. (1978) in *Centrifugal Separations in Molecular and Cell Biology* (Birnie, G. D., & Rickwood, D., Eds.) Chapter 3, Butterworth, London.
Sajdera, S. W., & Hascall, V. C. (1969) *J. Biol. Chem. 244*, 77.
Sartory, W. K. (1969) *Biopolymers 7*, 251.
Sartory, W. K., Halsall, H. B., & Breillat, J. P. (1976) *Biophys. Chem. 5*, 107.
Schachman, H. K. (1959) *Ultracentrifugation in Biochemistry*, Academic Press, New York.
Schumaker, V. N. (1967) *Adv. Biol. Med. Phys. 11*, 245.
Schumaker, V. N., & Rosenbloom, J. (1965) *Biochemistry 4*, 1005.
Steensgaard, J., Moller, N. P. H., & Funding, L. (1978) in *Centrifugal Separations in Molecular and Cell Biology* (Birnie, G. D., & Rickwood, D., Eds.) Chapter 5, Butterworth, London.
Svensson, H., Hagdahl, L., & Lerner, K. D. (1957) *Sci. Tools 4*, 1.
Williamson, R. (1971) in *Separation in Zonal Rotors* (Reid, E., Ed.) p Z-2.6, University of Surrey Press, Guildford, U.K.

Urea Dependence of Thiol–Disulfide Equilibria in Thioredoxin: Confirmation of the Linkage Relationship and a Sensitive Assay for Structure†

Tiao-Yin Lin and Peter S. Kim*
Whitehead Institute for Biomedical Research, Nine Cambridge Center, Cambridge, Massachusetts 02142, and Department of Biology, Massachusetts Institute of Technology, Cambridge, Massachusetts 02139

Received January 10, 1989; Revised Manuscript Received February 16, 1989

ABSTRACT: Thioredoxin contains a single disulfide bond that can be reduced without perturbing significantly the structure of the enzyme. Upon reduction of the disulfide, protein stability decreases. We have experimentally tested the expected linkage relationship between disulfide bond formation and protein stability for thioredoxin. In order to do this, it is necessary to measure the equilibrium constant for disulfide bond formation in both the folded and unfolded states of the protein. Using glutathione as a reference species, we have measured the equilibrium constant for forming the disulfide bond (effective concentration) in thioredoxin as a function of urea concentration. As a control, we show that urea per se does not interfere with our measurements of thiol–disulfide equilibrium constants. Comparison of the values obtained for disulfide bond formation in the folded and unfolded states with the free energies for unfolding oxidized and reduced thioredoxin using circular dichroism confirms the expected linkage relationship. The urea dependence of thiol–disulfide equilibria provides a sensitive assay for folded structure in peptides or proteins. The method should also be useful to evaluate the stabilizing or destabilizing effect of natural or genetically engineered disulfides in proteins. In future work, the effects of amino acid substitutions on disulfide bond formation could be evaluated individually in the native and unfolded states of a protein.

A useful way to think about thermodynamic linkage relationships in protein stability is to consider the effective concentrations of specific interactions in the protein (Creighton, 1983). Effective concentrations represent a ratio of equilibrium or rate constants for otherwise identical intra- and intermolecular reactions. The concept of effective concentrations, used to explain the chelate effect in inorganic chemistry (Schwarzenbach, 1952; Adamson, 1954), is recognized as a useful concept in enzymology (Page & Jencks, 1971). Ef-

† This research was supported by grants from the NIH (GM37241) and the Biotechnology Process Engineering Center at MIT (NSF CDR-8803014).
* Address correspondence to this author at Whitehead Institute for Biomedical Research.

0006-2960/89/0428-5282$01.50/0